Journal of Chemistry of Goods and Traditional Medicine

J Chem Good Trad Med, Volume 4, Issue 4, 2025 Chemistry of Goods

SYNTHESIS AND X-RAY DIFFRACTION ANALYSIS OF PERMEABLE POLYMER AND METAL OXIDE NANOCOMPOSITE MATERIALS FOR GAS SENSORS

Otabek A. Kuchkarov

Samarkand State Pedagogical Institute, Acting Associate Professor of the Department of Chemistry, PhD

https://orcid.org/0000-0002-6692-9352

E-mail: o-kuchkarov2018@mail.ru

DOI: https://doi.org/10.55475/jcgtm/vol4.iss4.2025.548

Keywords:

Polyaniline, tungsten oxide, tin oxide, triethylamine, semiconductor, gas-sensing material, sensor

Abstract

Flexible films of polyaniline-metal oxide hybrid nanocomposites were chemically synthesised via the oxidation-reduction process of aniline using ammonium persulfate (APS) as an oxidising agent in the presence of HCl. It was confirmed that the PANI/WO_3 nanocomposite was formed from monoclinic WO_3 oxide. The X-ray spectrum of the PANI/SnO_2 nanocomposite exhibited relatively broadened peaks compared to the standard X-ray diffractogram of SnO_2 oxide, indicating that a significant portion of the characteristic SnO_2 peaks became amorphous due to the PANI matrix. The PANI/(WO_3+SnO_2) composite material was identified as a triethylamine-sensitive gas-sensing material.

How to Cite

Kuchkarov, O. A. (2025). SYNTHESIS AND X-RAY DIFFRACTION ANALYSIS OF PERMEABLE POLYMER AND METAL OXIDE NANOCOMPOSITE MATERIALS FOR GAS SENSORS. Journal of Chemistry of Goods and Traditional Medicine, 4(4), 66-86. https://doi.org/10.55475/jcgtm/vol4.iss4.2025.548

Introduction. Conductive polymers are among the most promising materials that can be used in the production of semiconductor sensors. The production of films from these materials is inexpensive and can be prepared easily and lightly, which is advantageous for sensor fabrication. Primarily, polymers are used in the form of thin films, whose main function is to enhance the sensitivity of the sensing device [1]. In general, polymers can be utilised in all types of sensors capable of operating at room temperature. By varying the type and amount of dopant, it is possible to obtain polymers with a wide range of electrical properties, ranging from insulators to semiconductors [2].

Electrically conductive polymers such as polypyrrole (PPy), polyaniline (PANI), polythiophene (PTh), and their derivatives have been used as sensing layers in gas sensors since the early 1980s [3]. The use of conductive polymers in gas analysers has long been an important research topic. The ease of synthesising these polymers and their sensitivity at room temperature enhance the advantages of the sensor [4].

The operating principle of gas sensors based on semiconducting polymers is primarily based on measuring electrical conductivity. The electrical conductivity of polyaniline films in a gaseous environment depends on the concentration of gaseous ammonia. They are excellent materials for developing chemical or electrochemical sensors [5].

Metal oxide gas sensors offer advantages such as being relatively inexpensive, durable, lightweight, long-lasting, and having fast response signals. Gas detection using metal oxide sensors is of great importance today. However, the necessity to operate at high temperatures (300–500 °C) often limits the use of this type of sensor [6]. Thus, the combination of nanoscale metal oxides and conductive polymers is an effective approach to solving the aforementioned problems. Due to their

nanoscale dimensions, nanocomposites with filler dispersion exhibit significantly improved properties compared to pure polymers or their traditional composites. These improvements include increased modulus and strength, reduced barrier properties, enhanced solubility, and thermal stability [7].

We can conclude that the synthesis of conductive polymers and metal oxide nanocomposite materials for gas sensors is a relatively understudied field. Therefore, investigating the principles of creating sensors based on tungsten, titanium, polyaniline, and metal oxides, along with analyzing their X-ray diffractograms, holds both theoretical and practical significance.

Experimental Section and Discussion of Results

Preparation of tungsten oxide nanoparticles via the sol-gel method. A 25 mL solution of 3 M nitric acid (HNO_3) was added dropwise to 35 ml of a 0.15 M sodium tungstate solution (Na_2WO_4) under vigorous stirring using a magnetic stirrer. The resulting yellow precipitate was aged for 30 days at 25 °C.

To obtain WO_3 nanoparticles, the resulting gel was dried at 100 °C for 24 hours and subsequently subjected to thermal treatment at 400–500 °C (Figure 1).



Figure 1. WO_3 nanoparticles obtained after thermal treatment of the gel at 400–500 °C.

Synthesis of PANI–WO_3 nanocomposite film.

Polyaniline nanoparticles were synthesised from aniline monomers via chemical oxidation polymerisation. 0.46 ml of aniline (redistilled before use) and varying mass ratios of tungsten(VI) oxide (WO_3) (mass% = 10, 20, 30, 40, and 50) were added to 25 ml of a 1 M HCl solution and stirred using a magnetic stirrer for 30 minutes, followed by 30 minutes of ultrasonic treatment. Simultaneously, 0.005 mol of ammonium persulfate ($(NH_4)_2S_2O_8$) was dissolved in a measured quantity of HCl solution under vigorous stirring for 30 minutes to obtain the $(NH_4)_2S_2O_8$/HCl solution. This $(NH_4)_2S_2O_8$/HCl solution was then added to the previously prepared mixture and kept at room temperature for 48 hours, after which it was filtered.

Fabrication of polyaniline–WO_3–SnO_2 (PANI/WO_3–SnO_2) sensor films

The synthesized WO_3 nanoparticles were mixed with SnO_2 nanoparticles to obtain a homogeneous mixture with different WO_3:SnO_2 molar ratios (5:95, 10:90, 15:85, 20:80, 25:75, and 30:70). Finally, PANI was blended into the WO_3:SnO_2 composite solution in a molar ratio of 2 mol PANI to 1 mol (0.5 WO_3:0.5 SnO_2). The resulting composite solutions were then deposited onto glass substrates (Corning) by spin-coating, maintaining a uniform film thickness of 300 nm for all samples. The as-prepared films underwent a pyrolysis process at 100 °C to remove volatile precursors. Subsequently, the films were stabilised by thermal annealing at 300 °C for 3 hours.

The XRD spectrum of the PANI/WO_3 nanocomposite based on polyaniline and WO_3 is presented in Figure 2. The spectrum shows intense diffraction peaks at 2θ = 23.1°, 23.6°, 24.3°, 26.6°, 28.8°, 33.9°, 34.1°, 35.5°, 41.8°, 47.2°, 48.3°, 49.9°, 53.4°, 54.8°, and 62.3°, corresponding to Miller indices (002), (020), (200), (120), (112), (022), (220), and (222) (JCPDS cards No. 71-2141, No. 83-0950). This confirms that the synthesised PANI/WO_3 nanocomposite is formed from monoclinic WO_3 oxide [8–9].

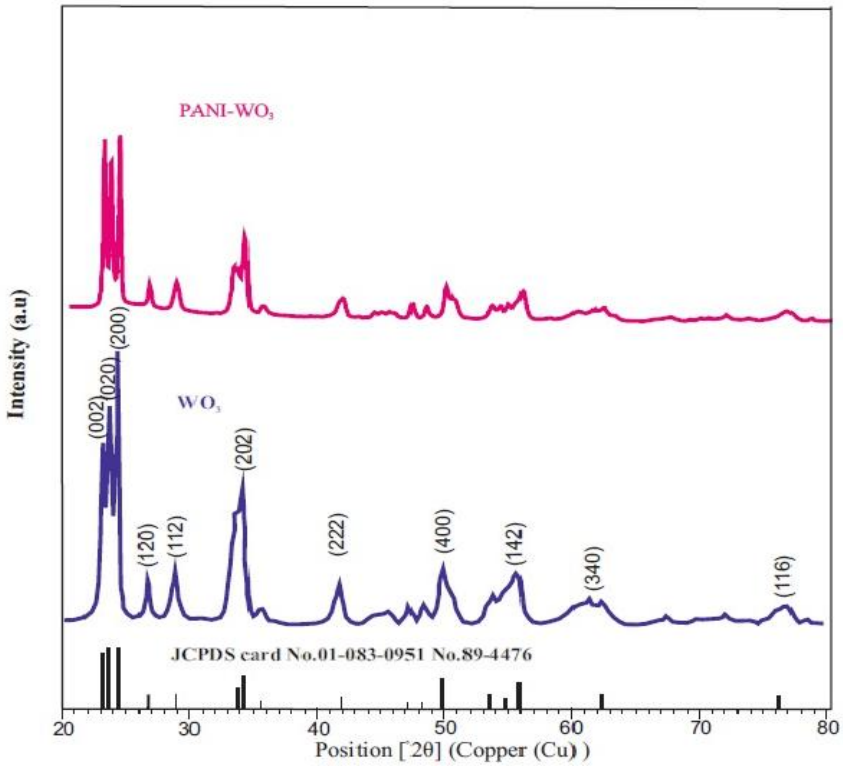


Figure 2. X-ray diffractograms of PANI/WO_3 and WO_3.

During the investigation, the WO_3 nanoparticle synthesis process involved calcination of the sample at 400–500 °C for 3 hours. It was determined that maintaining the calcination temperature above 450 °C leads to the formation of a stable monoclinic structure [8]. The average crystallite size is a crucial parameter influencing the properties of metal oxide nanostructures and was calculated using the Debye–Scherrer formula:

$$\mathbf{D = k\lambda / (\beta \cos\theta)} \quad (1)$$

where:

D = Crystallite size (nm)

K = 0.9 (Scherrer constant)

Λ = 0.15406 nm (X-ray source wavelength)

β = FWHM (full width at half maximum) in radians

θ = Diffraction angle in degrees

Based on the primary peaks observed in the X-ray diffraction (XRD) spectrum of the polyaniline and WO_3 nanocomposite—specifically at 23.1° (002), 23.6° (020), 24.3° (200), and 26.6° (120)—the average crystallite sizes were calculated as presented in Table 1. The results indicate that the average crystallite sizes corresponding to these major peaks are 35.67 nm, 36.82 nm, 40.42 nm, and 21.27 nm, respectively.

Table 1.

Average crystallite sizes calculated from the primary peaks observed in the X-ray diffraction (XRD) spectrum of the polyaniline and WO_3 nanocomposite.

Diffraction Angle Pos. [°2θ]	FWHM of Diffraction Peaks [°2θ]	Average Crystallite Size D (nm)
23.1	0.2373	35.67
23.6	0.2301	36.82
24.3	0.2099	40.42
26.6	0.4007	21.27

Analysis of Table 1 confirmed that the average crystallite sizes corresponding to the identified primary peaks are 35.67 nm, 36.82 nm, 40.42 nm, and 21.27 nm, respectively.

The spectrum presented in Figure 3 reveals the presence of diffraction peaks in the nanocomposite at 2θ = 26.2°, 33.9°, and 51.6°, corresponding to the (110), (101), and (211) planes, respectively (JCPDS card No. 41-1445). This confirms that the crystal possesses a simple tetragonal structure.

However, upon comparing the X-ray spectrum of the PANI/SnO_2 nanocomposite with the standard X-ray diffractogram of SnO_2 oxide, we observed a relative broadening of the peaks. This indicates the presence of tin oxide within the polyaniline matrix. Furthermore, it was determined that a significant portion of the characteristic SnO_2 peaks exhibits an amorphous nature due to the influence of the PANI matrix.

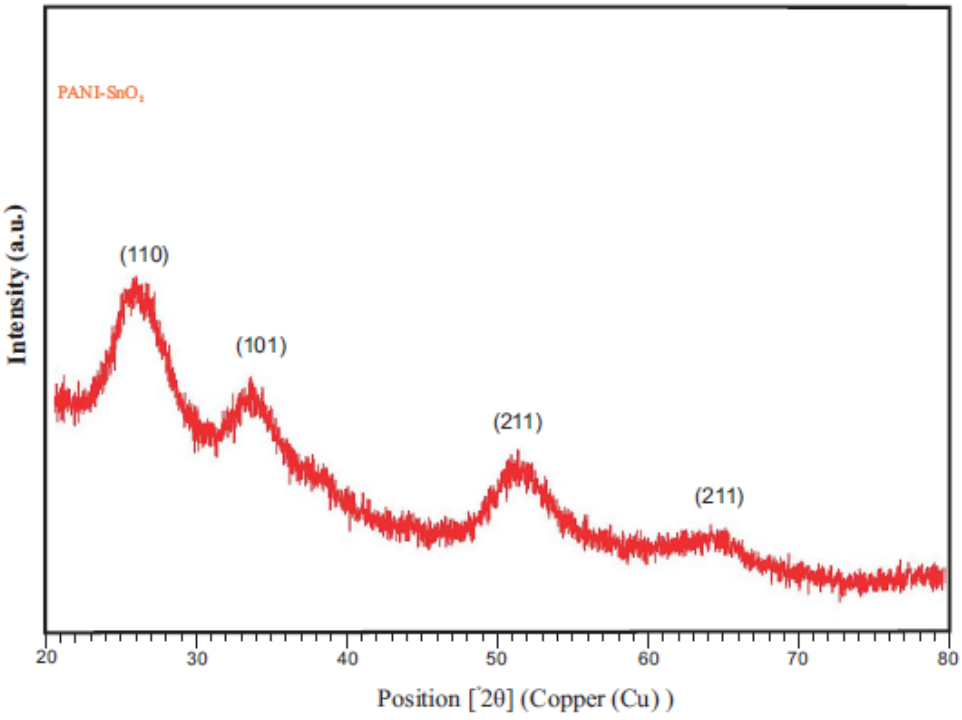


Figure 2.9. X-ray diffractogram of PANI/SnO_2.

Furthermore, the average crystallite size was determined using the Scherrer equation (1), and was found to be 4.87 nm and 5.07 nm, respectively (Table 2).

Table 2.

Diffraction Angle Pos. [°2θ]	**FWHM of Diffraction Peaks [°2θ]**	**Average Crystallite Size D (nm)**
26.2	1.75	4.87
33.9	1.7	5.07

Table 3 presents the dependence of sensor performance indicators on the composition of the gas-sensing material for triethylamine (TEA) detection (n=5, P=0.95).

Table 3.

Dependence of sensor performance indicators on the composition of the gas-sensing material for triethylamine (TEA) detection (n=5, P=0.95).

/r	Composition of Gas-Sensing Material	Sensor Signal for TEA, (mV),			**Dynamic Parameters (s)**		Sensitivity coefficient (S)
		x ±Δx		S r*10^2	**Response Time (t_{90})**	**Recovery Time (t_{10})**	
	PANI	6 ±0,02	0,016	0,27	17 1	20 5	1,0
	PANI+WO_3	27 ±0,04	0,032	0,12	13 4	18 8	5,3
	PANI+SnO_2	37 ±0,05	0,04	0,11	89	15 1	2,4
	PANI+TiO_2	16 ±0,03	0,024	0,15	10 9	16 3	4,3
	PANI/(WO_3+SnO_2)	55 ±0,06	0,048	0,09	51	78	7,9
	PANI/(WO_3+TiO_2)	42 ±0,05	0,04	0,10	29	10 1	8,2
	PANI/(SnO_2+TiO_2)	49 ±0,04	0,032	0,07	42	95	7,3

The data in the table reveal the following order of sensor sensitivity for TEA detection: **PANI/(WO_3+SnO_2) > PANI/(SnO_2+TiO_2) > PANI/(WO_3+TiO_2) > PANI+SnO_2 > PANI+WO_3 > PANI+TiO_2 > PANI.** (Sensors are listed in descending order of their sensitivity for amine detection at a room temperature of 20-30°C).

Based on these results, the sensor based on **PANI/(WO_3+SnO_2)** is characterized by the best overall parameters for TEA detection. Consequently, the **PANI/(WO_3+SnO_2)** nanocomposite was selected as the gas-sensing material for the triethylamine sensor in subsequent experiments.

Conclusions

Flexible films of polyaniline-metal oxide hybrid nanocomposites were synthesized via chemical oxidation polymerization using ammonium persulfate (APS) as an oxidizing agent and HCl, through the oxidation-reduction process of aniline. It was confirmed that the PANI/WO_3 nanocomposite was formed from monoclinic WO_3 oxide. Comparison of the X-ray spectrum of the PANI/SnO_2 nanocomposite with the standard X-ray diffractogram of SnO_2 oxide revealed a relative broadening of the diffraction peaks. This broadening indicated that a significant portion of the characteristic SnO_2 peaks possessed an amorphous nature due to the influence of the PANI matrix. The PANI/(WO_3+SnO_2) composite material was identified as a suitable gas-sensing material for the triethylamine sensor.

The developed TEA sensors are not inferior to renowned foreign counterparts in terms of accuracy and reproducibility, and are recommended for detecting TEA over a wide range of concentrations in air and industrial gases at room temperature. The sensor fully complies with GOST requirements established for devices of this category.

References

1. Giselle Jiménez-Cadena, Jordi Riu and F. Xavier Rius, Gas sensors based on nanostructured materials, Analyst, 2007, 132, – P. 1083–1099

2. Ekarat Detsri, Stephan Thierry Dubas, Interfacial Polymerization of Water- Soluble Polyaniline and Its Assembly Using the Layer-By-Layer Technique, Journal of Metals, Materials and Minerals. Vol.19. -2009. No.1 – P. 39-44,

3.Hua Bai and Gaoquan Shi, Gas Sensors Based on Conducting Polymers, Sensors -2007, 7, – P 267-307.

20. Ghenadii Korotcenkov, Chemical Sensors Comprehensive Sensor Technologies: Volume 4 Solid State Devices, “Chap. 1 - //Introduction to Chemical Sensor Technologies// 2011.– P 1-38.

4. Hatchett DW, Josowicz M., Composites of Intrinsically Conducting Polymers as Sensing Nanomaterials, Chem Review, Volume: 108, Issue: 2, -2008. – P 746-769.

5. George F. Fine, Leon M. Cavanagh, Ayo Afonja and Russell Binions, Metal Oxide Semi-Conductor Gas Sensors in Environmental Monitoring, Sensors 2010, -P. 5469-5502.

6. Arunkumar Lagashetty and A. Venkataraman, Polymer Nanocomposites, Resonance: Volume 10, Number 7 (2005), – P. 49-57.

7. Séverin N’goran EROI, Aimé Serge Ello, Donourou Diabate, Diby Benjamin Ossonon and Jocelin Martial YaO_3, Catalytic activity of using tungsten oxide with hydrogen peroxide for methyl orange degradation, African Journal of Pure and Applied Chemistry, Vol. 14(4), -P. 69-80, DOI: 10.5897/AJPAC2019.0827

8. R.Hatel, M. Baitoul, Nanostructured Tungsten Trioxide (WO_3): synthesis, structural and morphological investigations, IOP Conf. Series: Journal of Physics: Conf. Series, 1292 (2019) 012014 doi:10.1088/1742-6596/1292/1/012014

9. Abdurakhmanov I. E., Kuchkarov O. A., Abdurakhmanov E. Gas sensitivityspeed of ammonia semiconductor sensors based on metal –oxide films SiO_2/TiO_2+ Fe_2O_3 //Rasayan Journal of chemistry. Vol.13. №. 3. 2020. pp. 1486-1490.doi.org/10.31788/RJC.2020. 1335718.

10. Journal of Chemistry of Goods and Traditional Medicine, Vol. 1, Iss. 4 , P. 52-69.

11. Zhai, C.B.; Zhu, M.M.; Jiang, L.N.; Yang, T.Y.; Zhao, Q.; Luo, Y.; Zhang, M.Z. Fast triethylamine gas sensing response properties of nanosheets assembled WO_3 hollow microspheres. Appl. Surf. Sci. 2019, 463, -P. 1078–1084.

12.Ma, Q.; Chu, S.S.; Liu, Y.; Chen, Y.; Song, J.C.; Li, H.; Wang, J.P.; Che, Q.D.; Wang, G.; Fang, Y. Construction of SnS2 /ZIF-8 derived flower-like porous SnO_2/ZnO heterostructures with enhanced triethylamine gas sensing performance. Mater. Lett. 2019, 263, -P. 452–455